Envelope Protection and Control Adaptation in Icing Encounters

Kishwar N. Hossain*, Vikrant Sharma*, Michael B. Bragg†, and Petros G. Voulgaris‡
University of Illinois at Urbana-Champaign

Abstract

The goal of this research was to improve the envelope protection capabilities of an aircraft in icing conditions. To accomplish this goal, open and closed loop envelope protection algorithms were developed to ensure the safe operation of an iced aircraft during both manual and autopilot modes of flight. The Iced Aircraft Envelope Protection system (IAEP), developed as a part of the Smart Icing Systems (SIS) research project at the University of Illinois, was based on data from wind tunnel tests, flight tests and iced aircraft simulations obtained from a six-degree-of-freedom computational flight dynamics model. The system consisted of estimative and predictive methods for approximating, and avoiding the envelope boundaries. Simulation results demonstrated that IAEP was capable of successfully avoiding incidents and accidents during flight in icing conditions. This paper includes a summary of the basic scheme of the longitudinal iced aircraft envelope protection system and a discussion of results obtained through simulation.

Nomenclature

FDC	Flight Dynamics and Control
IAEP	Iced Aircraft Envelope Protection
IPS	Ice Protection System
PAH	Pitch Attitude Hold
SIS	Smart Icing System
SPS	Stall Protection System
a	acceleration
C_L	aircraft lift coefficient
C_{L0}	lift coefficient at zero angle of attack
$C_{L\alpha}$	lift curve slope
$C_{L\max}$	maximum lift coefficient
ΔC_L	change in aircraft lift coefficient
F	force
k_i , k_θ	controller gains
L	rolling moment
M	pitching moment
m	mass
N	yawing moment
p	rate of roll
q	rate of pitch
r	rate of yaw
u	x-component of velocity
$\bar{u}$	control vector
v	y-component of velocity
w	z-component of velocity
X	x-component of resultant aerodynamic force
$\bar{x}$	state vector
Y	y-component of resultant aerodynamic force
y_p	envelope parameter vector
$y_{p_{limit}}$	envelope parameter limit vector
Z	z-component of resultant aerodynamic force
α	angle of attack
α_{trim}	trim angle of attack
β	sideslip angle
δ_e	elevator angle
δ_a	aileron angle
δ_r	rudder angle
δ_p	power parameter
η	icing parameter
ψ	yaw angle
θ	pitch angle
ϕ	bank angle

1. INTRODUCTION

Aircraft performance, stability and control can change significantly during an icing event. These changes, particularly the degradation in aircraft

---

* Graduate Research Assistant, Department of Aeronautical and Astronautical Engineering, Member AIAA.
† Professor and Head, Department of Aeronautical and Astronautical Engineering, Associate Fellow AIAA.
‡ Associate Professor, Dept. of Aero. and Astro. Eng. and the Coordinated Science Lab., Member AIAA.

control, have resulted in aircraft incidents and accidents. For commercial aircraft, where revenue and schedules must be maintained, better systems are needed to allow the vehicle to operate safely under these conditions. In order to achieve this, NASA, the University of Illinois and The Ohio State University initiated the Smart Icing Systems research program in 1998. This research program was originally reviewed and explained by Bragg et al. in 1998[1] and a more recent program review was presented in 2002.[2] The concept of this program was to develop a system for in-flight measurement of the effect of ice on performance and control and to use this information to control the Ice Protection System (IPS), perform envelope protection, and adapt the flight controls. This paper deals with the envelope protection aspect of the project.

The flight envelope of an aircraft typically maps the combinations of altitude and velocity that the aircraft has been designed to withstand.[3] Other restrictions to the flight envelope may include the aerodynamic and structural limits of the aircraft. Envelope protection is the term used to describe the safety measures installed in an aircraft to ensure that it is flown within its flight envelope.

Envelope protection is an integral aspect of flight safety operations. All aircraft are equipped with some form of envelope protection, automatic or manual. Commercial aircraft such as the Boeing 777 and Airbus 320 take advantage of the fly–by-wire control systems using preset limits for parameters such as the angle of attack, bank angle, etc. [4] Commuter aircraft, such as the ATR 72, are equipped with stall protection systems (SPS) to prevent the pilot from exceeding preset limits.[5]

In icing, there is usually performance degradation due to ice accretion on the wings, tail, struts and other parts of the aircraft. Hence, the clean-aircraft preset envelope limits are usually reduced and there is an increased chance of incidents and accidents if the pilot or autopilot operates the aircraft close to the clean flight envelope. For example, in the 1997 Comair accident the Safety Board concluded that the stall warning system installed in the accident airplane did not provide an adequate warning to the pilots because ice contamination was present on the airplane's airfoils and the system was not designed to account for aerodynamic degradation or adjust its warning to compensate for the reduced stall warning margin caused by the ice.[6]

Due to icing related incidents and accidents the envelope protection systems aboard some aircraft were modified to account for the performance degradation due to ice accretion. For example, in the ATR 72 the SPS operates in conjunction with the IPS to reduce the angle of attack limit for stick shaker from 18.1^o to a predetermined value of 11.2^o in icing conditions.[5] However, this value is not modified based on the actual ice accretion, but on the ice accretion determined to be most critical during the certification process. If a more severe accretion occurs, the aircraft may stall or loose control at a much lower angle of attack. For example, in the ATR accident of 1994 the roll anomaly occurred at an angle of attack of 5^o.[5] Thus it is evident that setting limits that do not change with the actual iced-aircraft situation may not successfully protect the aircraft from violating its flight envelope.

Thus, the objective of the SIS envelope protection development effort was to design an envelope protection system that would provide flight envelope protection based on the characterization of the actual effect of the ice on the aircraft. The IAEP should also inform the pilot or autopilot of the modified envelope in sufficient time to take preventive/corrective measures. The purpose of this paper is to discuss the development of the IAEP.

The concept of an envelope protection system that adjusts or adapts to current aircraft conditions is relatively new. However, Horn et al.[7] have reported on such a system to provide enhanced cueing of the envelope limits of a rotorcraft to the pilot. They utilized the concept of dynamic trim, "a dynamic flight condition that the pilot is likely to sustain over several seconds in order to maneuver the aircraft,"[7] along with neural networks to predict if the aircraft would exceed its flight envelope during the course of a maneuver. In this method, a multi-layered feed-forward neural network was applied to approximate the values of the envelope parameters using information from measured aircraft states and control deflections as inputs. In other words, the neural network was trained to solve the following equation

$$\bar{y}_p = f(\bar{x}_m, \bar{u}) \tag{1}$$

where $\bar{y}_p$ are the envelope parameters to be limited and $\bar{x}_m$ and $\bar{u}$ are the aircraft state vector and control vector, respectively. The training was carried out using aircraft state data covering the entire flight envelope. The data were obtained from simulations using modified trim routines that generated trim data in quasi-steady maneuvers. The output from the neural network was compared to the limit value of the envelope parameter to calculate the "critical

control margin" used to determine the amount of force-feedback to be relayed to the pilot.

During the initial stages of the open loop IAEP research an attempt was made to apply the method outlined by Horn et al.[7] to icing. Merret et al. proposed the basic formulation in an AIAA conference paper[8] in 2002. Following the proposal, FDC[9] simulations were run to obtain dynamic trim values for the Twin Otter, the icing research aircraft used by NASA Glen. However, simulation results showed that a dynamic trim state as defined by Horn et al. did not exist for the Twin Otter. The aerodynamic angles showed considerable oscillations throughout the maneuvers studied. From the analysis of the short period and phugoid responses of the aircraft it was determined that the Twin Otter was not sufficiently damped to achieve dynamic trim in a reasonable time. Thus an alternative method was developed based on the near-real-time solution of the equations of motion to obtain predictions of the envelope parameter at a future point in time. This method will be discussed in further detail in section 2.2. However, the closed loop system uses a similar system as described by Horn et al., with the exception that it uses a table look-up method to sort through pre-obtained simulation data to find the maximum reference input that can be issued to obtain the desired flight path without exceeding the safe flight envelope.

2. ICED AIRCRAFT ENVELOPE PROTECTION METHODOLOGY

The idea of the IAEP system is to provide information to be used to limit the control deflections of an aircraft so that it remains within its flight envelope. For the manual, open-loop mode, a prediction scheme was thus designed to inform the pilot if the aircraft was anticipated to exceed the limits of the operating envelope. For the autopilot mode, a scheme based on limiting the steady state values of the critical parameters was developed so that the aircraft would efficiently follow the flight path specified by the pilot as closely as possible without exceeding the safe-flight envelope.

The critical parameters are defined in this study as those that are constrained by aerodynamic boundaries. The excursion of these parameters beyond their limit values may result in loss of aircraft control. During the formulation of the IAEP, a vector consisting of the critical parameters was defined as the envelope vector, $\overline{y}_p$.[7] The limits of the envelope vector, i.e. the maximum and minimum allowable values of the critical parameters at the given icing condition, were defined as functions of the icing parameter η[10]:

$$\overline{y}_p = \overline{y}_p(\overline{x}, \overline{u}, \eta) \tag{2}$$

$$\overline{y}_{p\lim} = \overline{y}_{p\lim}(\eta) \tag{3}$$

Then the envelope protection problem was simplified to constraining control inputs (whether in open- or closed-loop) at each time instant so that the critical parameters remained within their bounds:

$$\overline{y}^{l}_{p\lim} \le \overline{y}_p \le \overline{y}^{u}_{p\lim} \tag{4}$$

Where $\overline{y}^{l}_{p\lim}$ and $\overline{y}^{u}_{p\lim}$ were the lower and upper limits on the critical parameter. These equations were key to the development of the IAEP since they described the dependence of the envelope limits on the icing parameter and expressed their bounds.

2.1 Critical Parameter and its Limit Boundary

From a review of icing incidents and accidents it was found that aerodynamically the iced aircraft needed protection from wing stall, horizontal tail stall, roll upset and loss of longitudinal and lateral control. For example, the ATR 72 accident of 1994 near Roselawn, Indiana was caused by roll upset, which resulted from the loss of roll control above a specific, but low, angle of attack.[5] Similarly the BA-3101 Jetstream accident of 1989 was attributed to "loss of control at low altitude" which may have been caused when the horizontal stabilizer stalled.[11]

Eventually IAEP is expected to provide protection from all the phenomena mentioned above. However, in this paper we address the development of a system for the prevention of wing stall only. In order to prevent stall the aircraft angle of attack must be maintained at a value lower than the stall angle limit. Thus, the aircraft angle of attack was chosen as the critical parameter in order to formulate the longitudinal envelope protection scheme.

Having identified the critical parameter, it was necessary to define its boundaries as a function of data expected to be available for an SIS equipped aircraft. In order to develop this capability, data spanning the entire envelope for different icing conditions was needed. However, at this time only very limited data were available on iced aircraft limits from icing flight tests. Hence, for this research a very basic method was developed to calculate the limits of the angle of attack using data obtained from wind tunnel tests performed at the University of Illinois. The analysis was intended to identify trends in the performance degradation of an airfoil caused by simulated ice-shapes. Better methods to establish

iced aircraft envelope critical parameters are needed before a full implementation of this method.

The key was to develop the capability to determine the stall limits based on data available at low AOA. The most promising trend was found in the comparison of ΔC_L at constant angle of attack with iced airfoil C_{Lmax} data. Figure 1 illustrates this trend at an angle of attack of 4^o. In this figure, C_{Lmax} was plotted against ΔC_L. ΔC_L was the difference between the lift generated by an airfoil with simulated ice and the clean airfoil at the specified angle of attack.

$$\Delta C_{L(\alpha=4^o)} = C_{L,iced(\alpha=4^o)} - C_{L,clean(\alpha=4^o)} \quad (5)$$

It is evident from the figure that there is an almost linear relationship between C_{Lmax} and ΔC_L. This linearity existed for angles of attack ranging from 0^o to 11^o. Hence, if the stall angle could be approximated as a function of C_{Lmax}, it would be viable to use the value of ΔC_L to calculate the stall limit at a trimmed angle of attack.

In order to do this, a linear relationship was assumed between the stall angle of attack and the C_{Lmax}.

$$\alpha_{\text{limit}} = \frac{C_{L\max} + C_{L_0}}{C_{L_\alpha}} \quad (6)$$

Then, it was possible to define the limit value of the angle of attack as shown in eq. (7).

$$\alpha_{\text{limit}} = f(\Delta C_L) \quad (7)$$

Therefore, this model could be used to approximate the limit boundary of the angle of attack when the aircraft is trimmed as low as 0^o.

The estimative module of IAEP was implemented in the SIS Icing Flight Simulator. A block diagram of the estimative IAEP is shown in Fig. 2. It was used to provide input to the stall indicators in the glass cockpit. Simulations have shown that the algorithm was successful in estimating the stall angle for different maneuvers and icing conditions.

2.2 Open Loop IAEP

The purpose of the open loop IAEP was to warn the pilot of an impending stall and potential loss of control in sufficient time to correct the situation. Thus it was necessary to develop a method to predict limit violations in the future using the available sensor information. Although the formulation proposed by Horn et al.[7] utilized the same concept, the idea of dynamic trim as described by Horn et al. was not applicable to the icing aircraft. Thus the neural net-based method developed for the rotorcraft could not be implemented in the current research. Instead an alternative scheme was used. In the method developed here the equations of motion were integrated forward in time starting at the current aircraft state to predict the value of the critical parameter in the future. The future values of the critical parameter were then checked for limit violation.

The equations of motion were functions of the state and control vectors and also the icing parameter as shown in eq. (8).

$$\dot{\bar{x}} = g(\bar{x}, \bar{u}, \eta) \quad (8)$$

The state vector as given included the inertial velocity components, the components of the inertial rotational velocity and the Euler angles.

$$\bar{x} = [u \quad v \quad w \quad p \quad q \quad r \quad \theta \quad \phi \quad \psi] \quad (9)$$

The control vector included the deflections of the control surfaces and the power.

$$\bar{u} = [\delta_e \quad \delta_a \quad \delta_r \quad \delta_{power}] \quad (10)$$

The forces and moments were calculated using a nonlinear model, which incorporated the effect of the ice accretion quantitatively through η. The contribution of the icing parameter η thus occurred through the calculation of the forces and moments, which included the effect of the ice accretion modeled using η. The nonlinear model was based on data obtained from wind tunnel experiments using a scaled model of the Twin Otter aircraft.[12]

The equations of motion of a rigid body are modeled through the nonlinear ordinary differential equations shown in equations (11) through (21). These equations were derived from applying the flat earth approximation where the effect of the rotation and the curvature of the earth were neglected. Details of the derivation can be found in Etkin.[13]

Force equations:

$$\dot{u} = \frac{1}{m}\left(X - mg\sin\theta - m(qw - rv)\right) \quad (11)$$

$$\dot{v} = \frac{1}{m}\left(Y + mg\cos\theta\sin\phi - m(ru - pw)\right) \quad (12)$$

$$\dot{w} = \frac{1}{m}\left(Z + mg\cos\theta\cos\phi - m(pv - qu)\right) \quad (13)$$

Moment equations:

$$I_x\dot{p} - I_{zx}\dot{r} = L + (I_y - I_z)qr + I_{zx}pq \quad (14)$$

$$I_y\dot{q} = M + I_{zx}(r^2 - p^2) + (I_z - I_x)rp \quad (15)$$

$$I_z\dot{r} - I_{zx}\dot{p} = N + I_{zx}qr) + (I_x - I_y)pq \quad (16)$$

Kinematics:

$$\dot{\phi} = p + q\sin\phi\tan\theta + r\cos\phi\tan\theta \quad (17)$$

$$\dot{\theta} = q\cos\phi - r\sin\phi \quad (18)$$

$$\dot{\psi} = (q\sin\phi + r\cos\phi)\sec\theta \quad (19)$$

Position equations:

$$L_{VB} = \begin{bmatrix} \cos\theta\cos\psi & \cos\theta\sin\psi & -\sin\theta \\ \sin\phi\sin\theta\cos\psi - \cos\phi\sin\psi & \sin\phi\sin\theta\sin\psi + \cos\phi\cos\psi & \sin\phi\cos\theta \\ \cos\phi\sin\theta\cos\psi + \sin\phi\sin\psi & \cos\phi\sin\theta\sin\psi - \sin\phi\cos\psi & \cos\phi\cos\theta \end{bmatrix} \quad (20)$$

The resultant aerodynamic forces X, Y and Z in equations (11) through (13) were functions of the state vector, and control vector, and the icing parameter.

The method proposed for the open loop IAEP is given as follows:

1. The equations of motion are integrated forward in time assuming current control values, eq. (10).
2. If the predicted future values of the critical parameters, $\overline{y}_p$, do not satisfy eq.(4) this information is made available to the pilot.
3. The system then does an inverse calculation to determine the maximum safe control deflection.
4. The pilot is informed of the limit through the use of hard or soft limits.

For the open-loop case, the IAEP algorithm was written to solve the equations of motion for a specified time window into the future. The following assumptions were made in order to obtain the solutions:

1. Constant atmospheric properties
2. Constant mass properties
3. Constant or linearly increasing control deflections

The current system was developed using MATLAB. However, the system is scheduled to be a part of the SIS icing simulator by the summer of 2003, in which case the algorithm will be converted to C++ code.

2.2.1 Results

Validation

The solution code written using the equations presented above was validated against FDC simulations and flight test data as shown in Figs. 3 and 4.

Figure 3 shows the aircraft angle of attack versus time for a 30 second FDC simulation. The Twin Otter simulation was started at an initial velocity of 136 knots and altitude of 7545 ft. The η was set at a constant value of 0.1. A step elevator input of 3^o was issued at 5 seconds. As seen from the plot, due to the elevator input, the α goes beyond its stall limit of 10.5^o.

The open loop IAEP prediction shown as symbols on Fig. 3 was initiated at 12 seconds into the flight. The IAEP solution was run for 5 seconds into the future. As seen from the plot, the IAEP solution corresponds quite well with the FDC result especially for the first 3 seconds. The slight divergence observed toward the 4^{th} second was attributed to the fact that $\overline{u}$ was kept constant during the solution. Hence, unlike the FDC simulation where the power changes due to the change in altitude, in the IAEP solution the power term remained constant. However, the difference between the FDC and IAEP solutions were within $1/2^o$ and it was found that the solutions always over predicted. Therefore, the IAEP provides a safe estimate of the future values of the critical parameter.

The IAEP solutions were also validated against Twin Otter flight test data. The flight data used in this validation was obtained from flight tests completed in February 2002 as a part of the Smart Icing Systems research project. Figure 4a is a plot of the θ response to the δ_e inputs plotted in Fig. 4b for flight test number 020213f, a morning flight in clean conditions.[14] In the time frame being studied here, a 0.25g doublet was initiated at a time of 4 seconds.

For the validation, the IAEP was run starting at 4 seconds, 5.2 seconds and 8 seconds as indicated by the arrows in Fig. 4a. The symbols in Fig. 4a correspond to the IAEP solutions. As seen in this figure, the IAEP solution initiated at 4 seconds performed well until 4.8 seconds but beyond that, the IAEP predicted a continuous increase in the pitch while there was a drastic pitch down in the flight test data. This was due to the fact that, a step elevator

was issued at 4.8 seconds in the flight test. This step was not modeled in the IAEP as illustrated in Fig. 4b where at 4.8 seconds there was a step increase in the elevator for the flight test but the IAEP elevator value remained constant at -3.8^o.

Similarly, the IAEP solution initiated at 5.2 seconds compares well to the flight test data till the 6^{th} second when another step elevator was issued in the flight test while the IAEP elevator value remained at a constant value of 2.8^o.

The last IAEP solution being discussed here was initiated at 8 seconds. As seen from Fig. 4b the flight elevator remained fairly constant during this time. As a result the IAEP solution matched almost exactly the pitch response of the Twin Otter as seen in Fig. 4a. However, toward the 11^{th} second the IAEP began to diverge. This was attributed to the fact that at this point, there was a slight increase in the power during flight, which was not modeled in the IAEP.

The Twin Otter flight test data and the IAEP solutions compared well when the control deflections remained constant. This suggested that the IAEP solutions could be used to estimate stall for the Twin Otter if they were run every second or less, in which case the changes in elevator would be modified at the beginning of each IAEP solution and thus accurate predictions could be made about the state of the aircraft.

Integration Time for IAEP Predictive Solutions

Once a method was formulated to predict the state of the critical parameter, some analysis was done to determine the lead-time needed for the aircraft dynamics to adjust to corrective control inputs and avoid stall. FDC results were obtained for situations where the iced aircraft with η values of either 0.1, 0.15 or 0.3, was initially trimmed at an altitude of 1640 ft and an elevator input was issued. The initial velocities for the simulations ranged from 97 knots to 116.6 knots. The elevator inputs included instantaneous step increases of 3^o and 6^o, and gradual ramped increases of 0.06^o/sec, 0.08^o/sec and 0.2^o/sec. The IAEP was run with integration times of 1 second, 3 seconds, 5 seconds and 10 seconds.

Figure 5 is a plot of a situation where a ramped elevator input of 0.08^o/sec was issued at 0 seconds. The angle of attack increased at a rate of 0.2^o/sec until it reached its limit of 6.8^o at 12.1 seconds. The initial trim velocity was 97.2 knots. The icing parameter η was constant at a value of 0.3. Also shown in this plot were the IAEP solutions with 1 second, 3 seconds, 5 seconds and 10 seconds integration times. In other words, the 1 second IAEP would predict for a second in the future while the 10 seconds IAEP would predict 10 seconds into the future. If the critical parameter limit were exceeded within the solution time, a modified elevator input would be issued at the time the IAEP was initiated. The initial points of the IAEP solutions were indicated on Fig. 5 by the arrows. As seen from this plot, when the modified elevator was issued, the angle of attack decreased instantaneously and stall was avoided. The same phenomenon occurred for all the integration times that were studied. It was also noted that the peak value of the angle of attack for the modified response did not exceed the initial IAEP value. Thus, even with a lead-time of 1 second, the aircraft dynamics adjusted to the modified control deflection to avoid stall. However, the increase in the elevator input studied in Fig. 5 was a rather mild one and hence step elevator inputs that generated higher angular rates were studied to verify that a 1 second prediction time was sufficient to avoid stall.

Figure 6 is a summary plot of the results obtained from one of the go around scenarios mentioned above. In the original FDC simulation for this case, the initial velocity was 116.6 knots. The icing parameter η was at a constant value of 0.2. The go around was initiated with a step elevator input of 3^o at 0 seconds. As a result the angle of attack increased and exceeded the stall limit of 10^o at a time of 8.8 seconds.

Included in the plot were the modified responses obtained from applying the open loop IAEP to the situation described above. As mentioned above, 4 different integration times were used for the IAEP. In Fig. 6 the curve labeled IAEP 1 sec corresponds to the response of the aircraft when stall was predicted with a 1 second lead-time and the elevator input was modified to a new value to avoid exceeding α_{limit}. Also shown in Fig. 6 are the modified responses from the 3 second, 5 seconds and 10 seconds lead-time cases.

From the results presented in Figs. 5 and 6 it was evident that the open loop IAEP was successful in avoiding stall. The fact that the IAEP was successful in avoiding stall in the severe icing conditions and in spite of the high angular rates, induced by a step elevator input indicated that it would be an effective method to use for envelope protection of an iced aircraft.

Another important conclusion that can be drawn from this study is that the integration time to be used for

the IAEP does not seem to be dependent on the aircraft dynamics or the proximity of the aircraft angle of attack to its limit value. The warning lead-time necessary to avoid stall is expected to depend primarily on pilot reaction time and other human factors issues. Thus determining the appropriate integration time, or the time IAEP looks forward in time to predict potential stall, is a topic for a future human factors study.

The Maximum Control Deflection

Having developed a warning system for the open loop IAEP, it was necessary to develop an algorithm to compute the maximum possible control deflection that could be applied without stalling the aircraft. A parallel for this was the "critical control margin" introduced by Horn et al.[7] However, since a neural net and the idea of dynamic trim were not utilized for the IAEP, an alternative method was needed to compute this maximum control deflection. However, it should be noted that the methodology discussed here was only a simple iterative scheme that was applied to obtain initial results. In the future a more sophisticated system will be developed to complete this task.

In this method, in order to avoid limit exceedence, the elevator input was modified at increments of 0.5^o to find the maximum control deflection. This is illustrated in Fig. 7. In the original FDC simulation shown in this figure, the initial trim velocity was 97.2 knots and the icing severity was kept constant at an η value of 0.2. A step elevator of 3^o was issued at 0 seconds. The IAEP was also initiated at 0 seconds. A limit exceedence was detected at this time and the IAEP angle of attack responses for different elevator inputs were checked for limit violation. In Fig. 7 the angle of attack responses from the different elevator inputs were shown. In this particular case it was found that the maximum possible elevator deflection was -0.97^o. Hence, the maximum step elevator input that could be applied for the given aircraft state was -0.97^o.

Although this method did give good results, it was cumbersome and time consuming. Currently research is continuing to device a more sophisticated method based on the linearized equations of motion.

2.3 Closed Loop IAEP

2.3.1 The Autopilot Model

The Closed Loop IAEP was developed for the pitch attitude hold mode of the autopilot. The pitch attitude mode was chosen as it is at the heart of the longitudinal control system of the aircraft. The function of this mode is to track the pitch angle commands issued by the pilot. The controller structure used for this purpose was obtained from Rauw [15] and is a PID controller. This autopilot structure was selected for the Twin Otter as it represents a standard configuration for an autopilot system. The Pitch Attitude Hold (PAH) mode controls the pitch angle by applying appropriate deflections of the elevator if the actual pitch angle differs from the desired reference value. The structure of the pitch attitude hold mode of the PID controller is shown in Fig. 8. The desired reference value of the pitch angle to be tracked is denoted by θ_{ref} . The pitch angle of the aircraft is fed back to ensure that the desired pitch angle is attained. A proportional and integral controller is applied in order to make sure that no steady state errors in the pitch angle will remain. As long as the error signal, $(\theta_{ref} - \theta)$, is not equal to zero, the signal from the integrator will increase, which leads to an increasing elevator deflection, thus eliminating the error. A feedback loop of the pitch rate q in response to the elevator has been included to compensate for the small decrease in damping of the short period mode due to feedback. In Fig. 8, the block aircraft dynamics contains the aircraft's dynamic equations. The block actuator dynamics are used to obtain the elevator deflection corresponding to the signal coming from the controller. k_i, k_θ and k_q are gains used by the controller and are scheduled in terms of the aircraft velocity obtained for good operation at different trim velocities under clean conditions. Table 1 shows the values for the gains at different aircraft speeds.

2.3.2 Envelope Limiting Using Steady-State Estimation

An envelope protection system built into an autopilot should be able to perform two functions: limit detection and limit avoidance. The system must detect the encroachment of an envelope limit, and then it must take measures to prevent the violation of the limit. Since there is a time lag between the reference input and the closed loop response, a limit avoidance cueing system based on instantaneous data may allow inputs that will take the response of the aircraft beyond the allowable limits and hence it would not be a reliable envelope protection system. Thus it is necessary to have a prediction lead-time, i.e., it is desirable that the limit detection algorithm estimate future values of a limited parameter in order to provide sufficient time margin for the autopilot system to react to it. Hence given the icing parameter value the envelope protection system should be able

to calculate the envelope limit, and based on those limits, identify the reference inputs to the autopilot beyond which the maximum response of the critical parameter will cross the limit in future. Then it should constrain the θ_{ref} inputs within these values.

As described before, the critical parameter chosen was the angle of attack, i.e. $y_p=\alpha$. The upper limit on y_p is the stall angle, i.e. $y_{\lim}^{u} = \alpha_{stall}$, whose values for different flying conditions and for different values of the icing severity (parameterized by η) is obtained as described in section 2.1. Here consider keeping only the critical parameter under the upper limit and ignore the lower limits. A practical approach of doing predictions based on steady state information is chosen. This has the advantage of not requiring substantial real-time calculations. It is also based on the case considered here where the PID controller used for the PAH autopilot the angle of attack response for step inputs achieves its maximum at steady state at all flight conditions. The idea is to obtain limits on the reference pitch angle values which are the input to the PAH autopilot so that the steady state angle of attack response stays less than the stall angle. The effective prediction lead-time that is achieved is the settling time of the step response.
Let the closed loop PAH model of the aircraft be described by the equation

$$\dot{\overline{x}} = g(\overline{x}, \overline{u} = \theta_{ref}, \eta) \qquad (23)$$

To check whether a particular input leads to exceeding the envelope limits, one has to run forward in time eq. (23) along with eq. (2), where $\overline{u}$ is defined inside eq. (23). Then the system must check, if the steady-state value of the angle of attack satisfies eq. (4) using eqs. (2) and (3). This constitutes, in principle, the natural basis of envelope protection schemes, i.e., one can (in flight) run forward eq. (2) assuming θ_{ref} is kept constant at its current value and check if the angle of attack limits will be violated. If so, one can accordingly reduce θ_{ref} to a value that keeps the aircraft in the envelope otherwise it is kept unaltered. So using this logic, limits on θ_{ref} values can be obtained for different flying conditions so that the angle of attack response stays within the stall limits. The next subsection describes the way this scheme was put into practice in MATLAB and SIMULINK and presents some simulation results describing successful envelope protection.

2.3.3 Envelope Protection Module based on Steady-State Analysis

Figure 9 shows the schematic of the autopilot system equipped with the envelope protection scheme. The EP module works in the following steps:

1. Obtains the stall angle value using the information on the current value of the icing parameter η available and flying condition as described in Section 2.1
2. Using this limit on the angle of attack it calculate the limit on θ_{ref}
3. Reduce the θ_{ref} input from the pilot to ensure it is inside the limit obtained in step 2.

The determination of limits on the reference pitch command is based on off-line data collected for different flying conditions. A series of reference pitch commands are issued for several flying conditions and different levels of icing and the steady-state values of the angle of attack for all situations are recorded in a variable along with the reference pitch commands, the trim velocity and the icing parameter value to which they correspond. This can be done in simulation or looking at the DC gain of the transfer function from the reference input to angle of attack for various η levels. The differences appeared to be small (at least when linear aerodynamics models, with nonlinear equations of motion, are considered). The steady-state angle of attack response at a given flying velocity and icing parameter η to a reference pitch command can then be obtained through these data by using 3-D interpolation. At any time instance, a quick iteration finds an estimate of the θ_{refmax} that will cause the steady-state response of the angle of attack to go beyond the given stall limit. With this function at hand, the mechanism for envelope protection works as follows: at any checking instance, the determined θ_{refmax} plus the current value of θ is compared with the θ_{ref} issued at the previous checking instance; if the latter is greater than the former then it is reduced down to equal the former. This check is done every 5 seconds. The procedure is depicted in Fig 10. As shown in Fig 10 every 5 seconds the EP module interpolates between data to obtain θ_{refmax} at the current flying conditions using the current velocity and η value. It then checks whether $\theta_{ref} > \theta_1 + \theta_{ref\max}$. If that is the case then it sets $\theta_{ref} = \theta_1 + \theta_{ref\max}$. This function was then incorporated into the autopilot part of the aircraft where it checks for the reference pitch command every five seconds and modifies it if it was greater

than the allowable reference pitch at that particular flying condition.

2.3.4 Simulation Results

In this section two different situations are considered, linear and nonlinear aerodynamics. In both cases, the overall model contained the nonlinear kinematics and dynamics.

Linear Aerodynamics Case

Two different scenarios are discussed in this subsection and the successful operation of the envelope protection module is demonstrated.

Case 1: The aircraft is initially trimmed at V = 50 m/s at a height of 2300 m with an icing level of η = 0.2. The stall limit at this icing level is an angle of attack of 11.7 degrees. A pitch-up command of 4 degrees is issued. Figure 11(a) shows the angle of attack response comparison for the case with the envelope protection module 'off' against the one with the envelope protection module 'on'. Clearly, for the case when the EP module is kept on, the angle of attack response does not violate the stall limit. This happens because the EP module manages to detect that the issued pitch up command is greater than the maximum allowable value at this flying condition and reduces it as shown in Fig. 11(c). The corresponding pitch response comparison is shown in Fig. 11(b).

Case 2: The aircraft is initially trimmed at a height of 2300 m at a velocity of 60 m/s under clean conditions. A pitch up command of 4 degrees is issued, ice starts to build and grows from η=0 at t=0 to η = 0.2 at t = 50s. As seen from the Fig. 12(a), the angle of attack response in the case where the envelope protection scheme is not operational crosses the stall angle limit. Note that the limit is dynamic because of the change in the icing severity. The angle of attack stall limit starts at 17.6 degrees under clean conditions and falls to 11.7 degrees by 50 seconds where the icing level reaches η = 0.2. In comparison the envelope protection scheme manages to sense the approaching stall angle dynamic limit and reduces the reference pitch value as shown in Fig. 12(c) to avoid the stall limit violation well in advance.

In both of these scenarios the response of the aircraft above the stall limit when the EP module is off is not realistic. That is, this 'benign' behavior of the aircraft in stall is solely due to the assumed linear aerodynamics model, which does not capture the post stall behavior. In that sense, these figures should be taken as a demonstration of successful angle of attack limiting when the EP module is on. A more realistic picture is given in the following section where a post stall nonlinear icing aerodynamics model is used.

Nonlinear Aerodynamics Case

Case 3: The aircraft is initially trimmed at a height of 2300 m at a velocity of 60 m/s under clean conditions. A pitch up command of 5 degrees is issued, ice starts to build and grows from η = 0 at t = 0 to η = 0.2 at t = 50 s. As seen from the Fig. 13(a), the angle of attack response in the case where the envelope protection scheme is not operational crosses the stall angle limit and enters the nonlinear regime. The autopilot response in the region seems to be oscillatory and there is stall as seen from Fig. 13(d) where the height of the aircraft falls in the case where the EP module is not incorporated. This indicates that it is dangerous to operate the autopilot under icing without the EP module. Note that the limit is dynamic because of the change in the icing severity. The angle of attack stall limit starts from 17.6 degree under clean conditions and falls to 11.7 degrees by 50 seconds where the icing level reaches η = 0.2. In comparison the envelope protection scheme manages to sense the approaching stall angle dynamic limit and reduces the reference pitch value to avoid the stall limit as shown in Fig. 13(c). Many other simulations were run and it was seen that the EP module performed well, keeping the aircraft response within the iced envelope.

3. SUMMARY AND CONCLUSIONS

The development of an envelope protection system for an iced aircraft was explored in this paper. The system developed is capable of estimating the stall limits in icing conditions and predicting if the aircraft will stall in the future.

Simulations showed that a prediction based envelope protection system can provide the pilot with enough lead-time to avoid icing related accidents and incidents, and that the solution of the equations of motion into the future is a viable method for a predictive envelope protection scheme. It was also found that a one second lead-time is sufficient for the aircraft dynamics to adjust to corrective control inputs and avoid incidents and accidents. Human factors research is necessary to determine the lead-time needed by a pilot to react to warnings issued and thus to set the time increment that the system uses.

The pitch attitude hold autopilot of the Twin Otter aircraft was modified to account for the effects of

icing. A standard PID controller was chosen with gains tuned with respect to the aircraft velocity. An envelope protection scheme using a practical approach of keeping the steady state response of the angle of attack within bounds was developed. In this approach, limits on the θ_{ref} values were obtained off-line at different flying conditions such that the steady state angle of attack response stayed within the stall limits. These data generated were then used to obtain a prediction lead-time for on-line simulations for cutting down the reference pitch inputs in order to avoid stall when the aircraft is in operation under the influence of ice accretion. The algorithm for the envelope protection module was presented and its operation was demonstrated through simulations.

ACKNOWLEDGEMENTS

This work was supported by a NASA Glenn grant NAG 3-21235. The authors would like to thank Mr. Tom Bond, Mr. Tom Ratvasky and Dr. Mark Potapczuk of NASA Glenn for their contributions. Several members of the Smart Icing Systems research group at Illinois contributed to this research including Dr. Sam Lee and Mr. Edward Whalen.

References

[1] Bragg, M.B., Perkins, W.R., Sarter N.B., Basar, T., Voulgaris, P.G., Gurbacki, H.M., Melody, J.W. and McCray, S.A., "An Interdisciplinary Approach to Inflight Aircraft Icing Safety," AIAA Paper No. 98-0095, Reno, NV, January 12-15, 1998.

[2] Bragg, M. B., Perkins, W.R., Basar, T., Sarter, N. B., Voulgaris, P. G., Selig, M., and Melody, J., " Smart Icing Systems for Aircraft Icing Safety," AIAA Paper No. 2002-0813, Reno, NV, Jan., 2002.

[3] Raymer, D., "Aircraft Design: A Conceptual Approach," AIAA Education Series, AIAA.

[4] North, M. D., "Finding Common Ground IN Envelope Protection Systems," Aviation Week & Space Technology, August 28, 2000.

[5] National Transportation Safety Board, "Aircraft Accident Report: Inflight Icing Encounter and Loss of Control Simmons Airlines, d.b.a. American Eagle Flight 4184 Avions de Transport Regional (ATR) Model 72-2122, N401AM, Roselawn, Indiana, October 31, 1994," Safety Board Report, *NTSB/AAR-96/01, PB96-910401, Volume 1,* July 1996.

[6] National Transportation Safety Board, "Aircraft Accident Report: In-flight Icing Encounter and Uncontrolled Collision with Terrain–Embraer EMB-120 RT, Monroe, Michigan January 9, 1997.

[7] Horn, J., Calise, A. J., Prasad, J. V. R., and O'Rourke, M., "Flight Envelope Cueing on a Tilt Rotor Aircraft Using Neural Network Limit Prediction," AHS 54th Forum, 1998

[8] Merret, J., Hossain, K., "Envelope Protection and Atmospheric Disturbances in Icing Encounters," AIAA Paper No. 2002-0814, Reno, NV, January 14-17, 2002

[9] Rauw, M., "FDC 1.3–A SIMULINK Toolbox for Flight Dynamics and Control Analysis," 1998.

[10] Bragg, M. B., Hutchinson, T., Merret, J., Oltman, R., and Pokhariyal, D., "Effects of Ice Accretion on Aircraft Flight Dynamics," AIAA Paper No. 2000-0360, Reno, Nv, Jan. 2000.

[12] Sharma, V., "Twin Otter Autopilot Analysis, Design and Envelope Protection for Icing Conditions," Master's Thesis, University of Illinois, Urbana-Champaign.

[13] Etkin, B., "Dynamics of Atmospheric Flight," John Wiley and Sons, Inc., New York, 1972.

[14] Ratvasky, Tom, (Private Communication), 2002.

[15] M. Rauw, "FDC 1.3 – A SIMULINK Toolbox for Flight Dynamics and Control Analysis,"1998.

Table 1. Gains used for the PAH autopilot

Velocity (m/s)	K_θ	K_i	K_q
40	-1.1	0.5	-0.1931
60	-0.9	0.5	-0.0631
80	-1.003	0.5	-0.3131

Table 2 Gain and Phase margins for the PAH autopilot at different velocities

Velocity (m/s)	Maximum θ_{ref} allowed (deg)
60	8.2
65	9.8
70	11.4
80	15.8

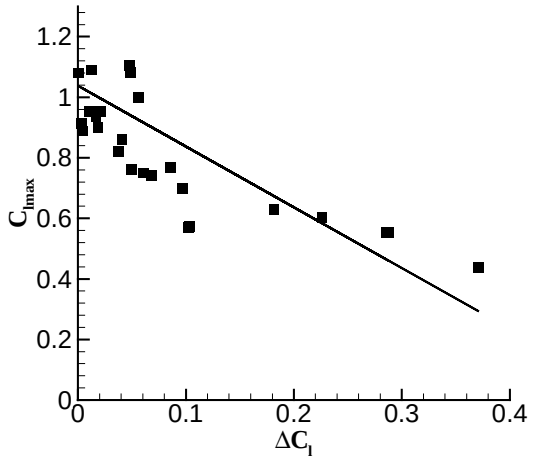

Fig. 1. Maximum Lift Coefficient as a Function of the change in lift at Constant α

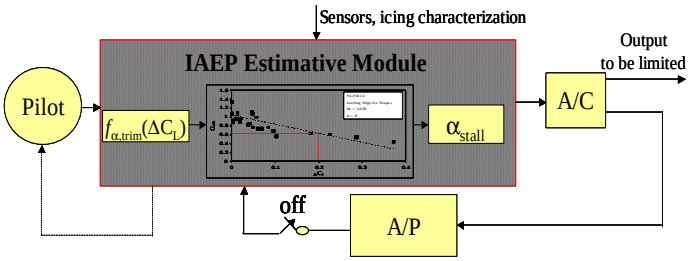

Fig. 2. Block Diagram of the Estimative IAEP

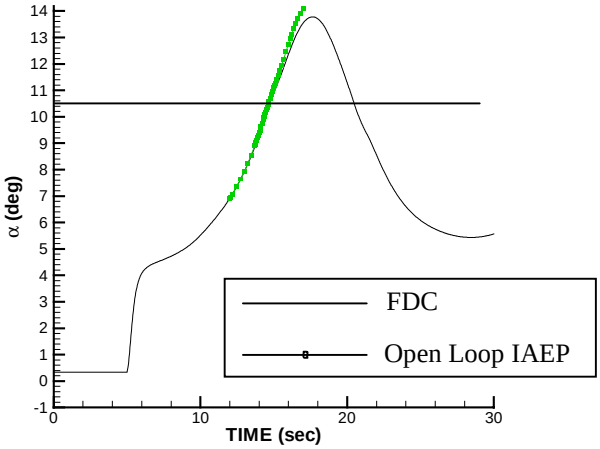

Fig. 3. Validation of Open Loop IAEP Prediction with FDC Result

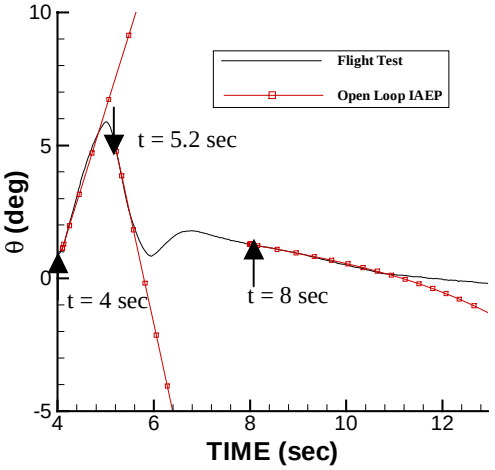

(a)

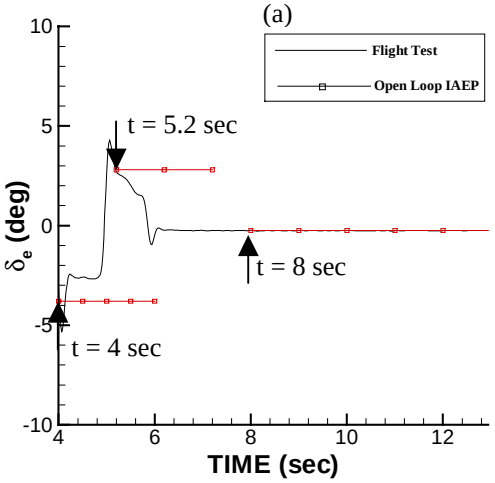

(b)

Fig. 4. Validation of Open Loop IAEP Prediction with Flight Test Data

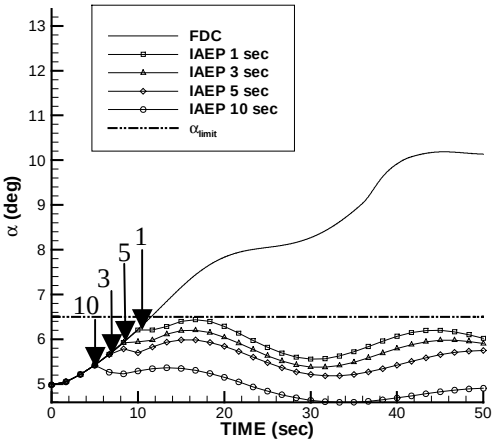

Fig. 5. IAEP Performance for different integration times for ramped elevator input.

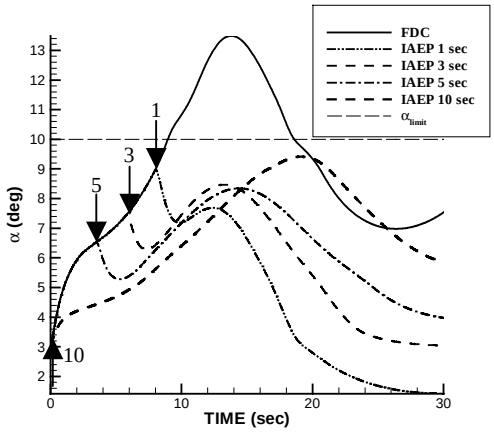

Fig. 6. IAEP Performance with different integration times for step elevator input

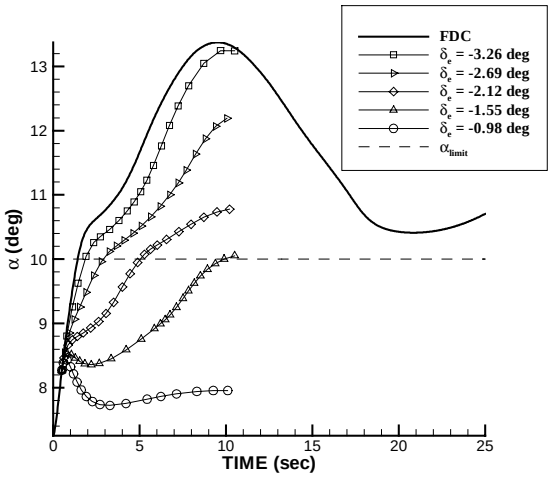

Fig. 7. Finding a control deflection.

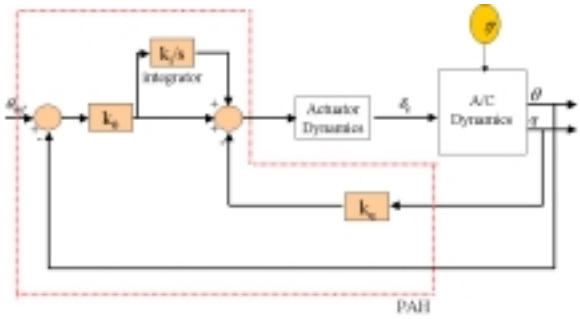

Fig. 8. The Block Diagram of the Closed Loop PAH Autopilot

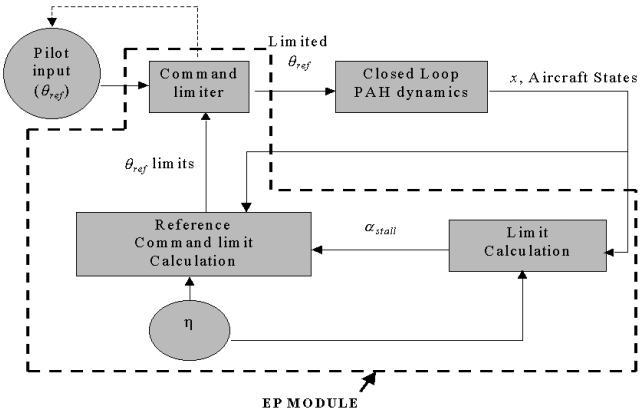

Fig. 9. Envisioned Envelope Protection System for the PAH autopilot

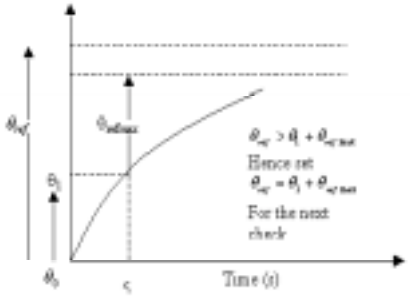

Fig. 10. Diagram of the Pitch response depicting the Envelope Protection input command-limiting scheme

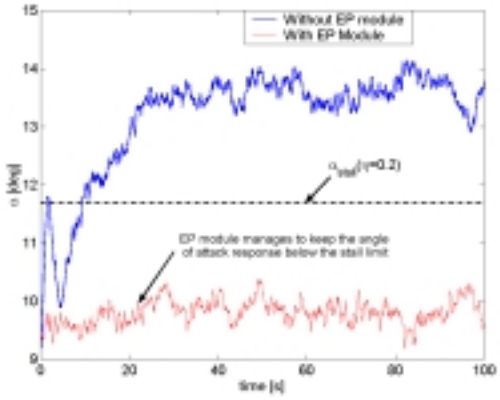

Fig. 11a. Angle of Attack Response

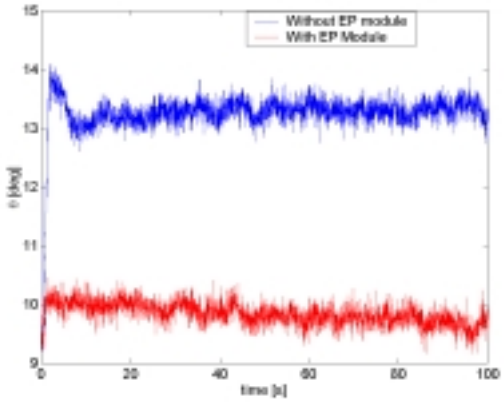

Fig. 11b. Pitch Response

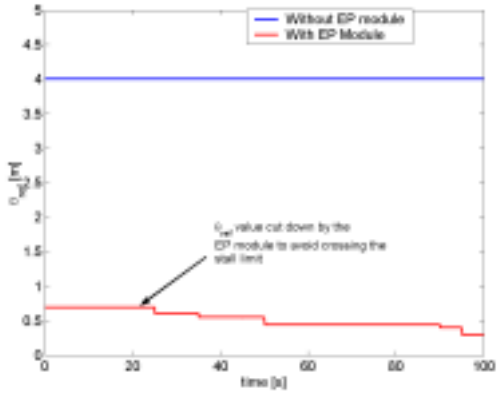

Fig. 11c. θ_{ref} Time History

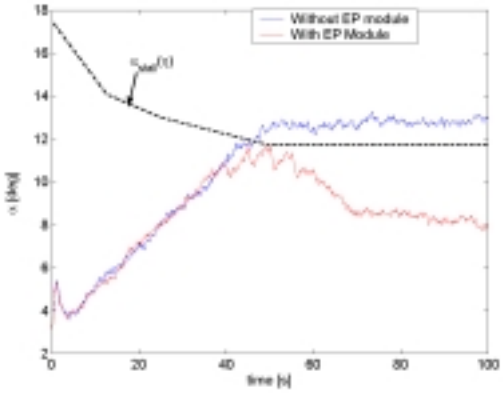

Fig. 12a. Angle of Attack Response

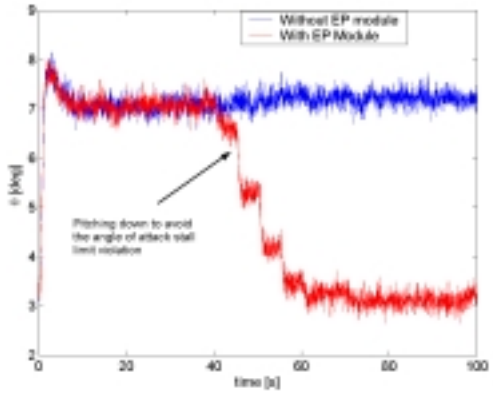

Fig. 12b. Pitch Response

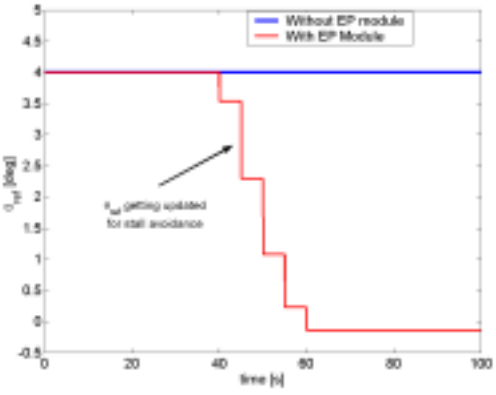

Fig. 12c. θ_{ref} Time History

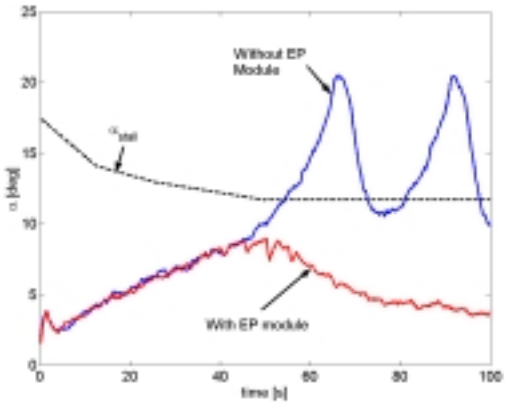

Fig. 13a. Angle of Attack Response

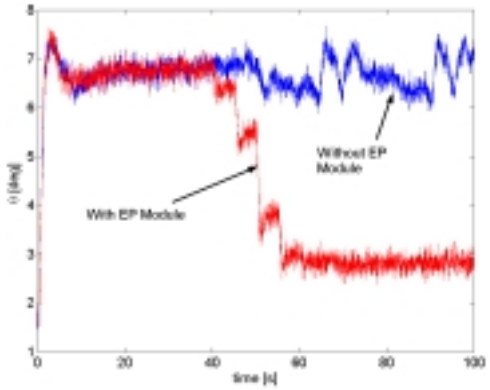

Fig. 13b Pitch Response

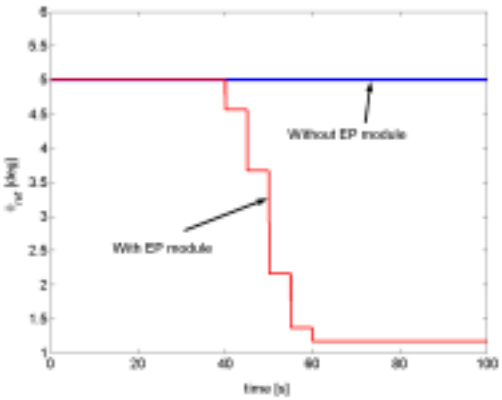

Fig. 13c. θ_{ref} Time History

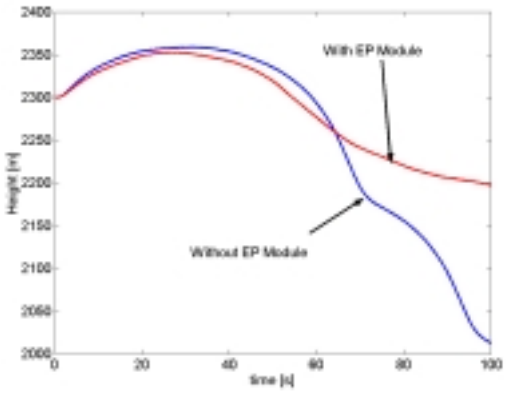

Fig. 13d. Altitude Response